Inorg. Chem. **2007**, *46*, 5904–5910

Spectroscopic Characterization of Hydroxylated Nanoballs in Methanol

Randy W. Larsen,* Gregory J. McManus, John J. Perry IV, Edwin Rivera-Otero, and Michael J. Zaworotko

Department of Chemistry, University of South Florida, 4202 E. Fowler Avenue, Tampa, Florida 33620

Received November 29, 2006

In this report, the photophysical properties of self-assembled $[Cu_2(5\text{-OH-bdc})_2L_2]_{12}$ [where $(5\text{-OH-bdc})^{2-}$ = 5-hydroxybenzene-1,3-dicarboxylate and L is a dimethyl sulfoxide, methanol, or water ligand] hydroxylated nanoballs (OH-nanoball) were examined in methanol using optical absorption and steady-state and time-resolved fluorescence methods. The optical spectrum of the OH-nanoball is dominated by ligand absorbance at 305 nm and a weaker Cu^{2+}-to-ligand charge-transfer transition at ~695 nm, which are distinct from the absorption of either the free ligand (~312 nm) or $Cu^{2+}(NO_3)_2$ (>750 nm) in methanol. The corresponding emission spectrum of the OH-nanoball originates from the emission of the ligand and is centered at ~360 nm with a shoulder at ~390 nm. The emission from the OH-nanoball is significantly quenched relative to the free ligand [$\Phi_{5-OH-H_2bdc} = 0.014$ and $\Phi_{OH-nanoball} = (5.6 \pm 0.5) \times 10^{-5}$]. The addition of bases such as imidazole results in an increase in the emission intensity of the OH-nanoball solution, indicating dissociation of the $[Cu_2(5\text{-OH-bdc})_2L_2]_{12}$ units. Although the mechanism of $(5\text{-OH-bdc})^{2-}$ quenching within the OH-nanoball is not clear, it is likely due to interactions between the ligand π system and the Cu d orbitals. Fluorescence polarization studies further suggest that the OH-nanoball retains a spherical shape in solution. This is evident by the fact that the fluorescence anisotropy of the nanoball is nearly identical with that of the free ligand, suggesting rapid energy transfer (homogeneous fluorescence resonance energy transfer) between ligands within the OH-nanoball.

Introduction

The synthesis of discrete nanometer-scale materials is of key importance for a wide array of applications including targeted drug delivery[1] (using "nanocapsules"), nanoscale machines,[2] nanooptical components[3] (nanoscale light-emitting diodes, lasers, etc.), and nanoscale sensing devices.[4] To date, a plethora of nanomaterials have now been synthesized and characterized including quantum dots, fullerenes, carbon nanotubes, solid metal nanospheres, and organic nanoclusters, to name only a few.[5] A wide array of metal−organic-based materials often referred to as coordination polymers, organic−inorganic hybrid materials, metal−organic networks, and metal−organic frameworks have been developed;[6] depending

* To whom correspondence should be addressed. E-mail: rlarsen@cas.usf.edu.

(1) (a) LaVan, D. A.; McGuire, T.; Langer, R. *Nat. Biotechnol.* **2003**, *21* (10), 1184−1191. (b) Hughes, G. A. *Nanomedicine* **2005**, *1* (1), 22−30. (c) Sahoo, S. K.; Labhasetwar, V. *Drug Discovery Today* **2003**, *8* (24), 1112−1120.

(2) (a) Craighead, H. G. *Science* **2000**, *290* (5496), 1532−1535. (b) Wang, Z. L. *J. Mater. Chem.* **2005**, *15* (10), 1021−1024. (c) Tsukruk, V. V. Molecularly assembled interfaces for nanomachines. In *Nanostructures: Synthesis, Functional Properties, and Applications*; Tsakalakos, T., Ovid'ko, I. A., Vasudevan, A. K., Eds.; NATO Science Series II Mathematics, Physics, and Chemistry; Kluwer Academic Publishers: Dordrecht, The Netherlands, 2003; Vol. 128, pp 95−109. (d) Balzani, V.; Credi, A.; Raymo, F. M.; Stoddart, J. F. *Angew. Chem., Int. Ed. Engl.* **2000**, *39* (19), 3348−3391.

(3) (a) Gvishi, R.; Narang, U.; Ruland, G.; Kumar, D. N.; Prasad, P. N. *Appl. Organomet. Chem.* **1997**, *11* (2), 107−127. (b) Sauer, J.; Marlow, F.; Schuth, F. Nanoporous materials for optical applications. In *Handbook of Advanced Electronic and Photonic Materials and Devices*; Nalwa, H., Eds.; Academic Press: New York, 2001; Vol. 6, pp 153−172. (c) Xia, Y.; Yang, P.; Sun, Y.; Wu, Y.; Mayers, B.; Gates, B.; Yin, Y.; Kim, F.; Yan, H. *Adv. Mater.* **2003**, *15* (5), 353−389. (d) Link, S.; El-Sayed, M. A. *Annu. Rev. Phys. Chem.* **2003**, *54*, 331−366. (e) Wang, Y.; Herron, N. *J. Phys. Chem.* **1991**, *95* (2), 525−532. (f) Wang, Y. *Acc. Chem. Res.* **1991**, *24* (5), 133−139.

(4) (a) Walt, D. R. *Nat. Mater.* **2002**, *1* (1), 17−18. (b) West, J. L.; Halas, N. J. *Annu. Rev. Biomed. Eng.* **2003**, *5*, 285−292. (c) Varghese O. K.; Grimes, C. A. *J. Nanosci. Nanotechnol.* **2003**, *3* (4), 277−293.

(5) (a) Drexler, K. E. *Nanosystems: Molecular Machinery, Manufacturing, and Computation*; John Wiley & Sons, Inc.: New York, 1992. (b) Rao, C. N. R.; Cheetham, A. K. *J. Mater. Chem.* **2001**, *11* (12), 2887−2894. (c) Rao, C. N. R.; Sen, R.; Govindaraj, A. *Curr. Opin. Solid State Mater. Sci.* **1996**, *1* (2), 279−284. (d) Schmid, G. *J. Chem. Soc., Dalton Trans.* **1998**, *7*, 1077−1082. (e) Kroto, H. W.; Allaf, A. W.; Balm, S. P. *Chem. Rev.* **1991**, *91* (6), 1213−1235. (f) *The Chemistry of Nanomaterials: Synthesis, Properties and Applications*; Rao, C. N. R., Müller, A., Cheetham, A. K., Eds.; Wiley-VCH GmbH & Co. KGaA: Weinheim, Germany, 2004.

10.1021/ic062268i CCC: $37.00
Published on Web 06/22/2007

upon the geometry and size of the metal−metal cluster and the organic ligands used, it is possible to design extended 2D or 3D frameworks[7] of known topologies and even discrete supermolecules[8] possessing nanometer-sized pores and/or cavities. These materials have enormous potential in gas storage and delivery, highly specific sensors, drug-delivery systems, single-cavity catalysis, small-molecule sensing, etc.

One of the advantages of metal−organic materials, such as the discrete nanoballs described herein, is that they are composed of spectroscopically active molecules. This is due to the fact that one of the key criteria for making rigid structures is the use of highly conjugated organic ligands including benzene di- and tricarboxylate derivatives, bipyridyls, etc. These ligands typically have well-characterized electronic properties including absorption and emission spectra, emission lifetimes, quantum yields, etc., originating from S_0 to S_n transitions (absorption) and S_1 to S_0 transitions (emission) in which the singlet states are derived from various mixtures of $\pi \rightarrow \pi^*$ excitations.[9] Because the electronic states of these chromophores are also sensitive to the local environment, the optical properties can serve as effective reporter groups for local perturbations in solvent, guest association, and local dielectric effects. In addition, metal coordination to conjugated ligands often results in the formation of metal-to-ligand as well as ligand-to-metal charge-transfer states that appear in the near-UV to near-IR region of the optical spectrum. For example, Cu^{2+}, which is one of the most commonly utilized transition-metal ions in metal carboxylate materials, typically displays charge-transfer transitions in the near-IR region involving the Cu 3d orbitals and either σ or π orbitals centered on the ligands.[10] These transitions are obviously sensitive to the nature of the ligands as well as to the ligand−metal geometry.

An interesting type of discrete metal−organic structure is the nanoball described herein because these materials have the potential for high solubility, the organic ligands can be easily functionalized, and they can be designed to have large interior cavities. These properties are ideal for interactions with biological molecules and for use as target-specific drug-delivery systems. Recently, a series of nanoscale molecules have been prepared based upon faceted polyhedra, namely, the *small rhombihexahedron*. Geometrically, the *small rhombihexahedron* consists of 12 squares linked through each of their four vertices at an angle of 120° in such a manner as to enclose space. In these nanoballs, the 12 square building units are, in fact, 12 $M_2(RCO_2)_4$ paddlewheel clusters[11] (where M is a metal ion and RCO_2 represents an organic carboxylate ligand). These 12 molecular squares are subsequently linked through the use of 24 benzene-1,3-dicarboxylate ligands at an angle of 120°, given that this is the angle subtended between the two carboxylates of the benzene-1,3-dicarboxylate ligand.[12]

Although a variety of transition metals can be utilized in forming the paddlewheel clusters and these nanoballs, the Cu^{2+} ion readily forms stable $Cu_2(RCO_2)_4$ and is one of the most prevalent metals utilized in these paddlewheel clusters (over 44% of all structures in the Cambridge Structural Database containing the $M_2(RCO_2)_4$ paddlewheel involve Cu^{2+}; *Conquest 1.8*, last updated Aug 2006).[13]

Using this design principle, a variety of nanoballs have been prepared using benzene-1,3-dicarboxylates substituted with various functional groups at the 5 position of the aromatic ring including amino, nitro, hydroxyl,[14a,b] dodecyloxy,[14c] sulfonato,[14d] methoxy,[14d] and *tert*-butyl ($M = Mo^{2+}$ rather than Cu^{2+})[14e] substituents. Self-assembled nanoballs contain solvent molecules [typically dimethyl sulfoxide (DMSO), pyridine, or methanol] axially coordinated to the Cu ions both on the exterior and interior of the nanoball. These nanoballs have relatively large molecular volumes (9.2−54.4 nm^3 depending upon the type of substitution on the aromatic ring) and internal cavity volumes of ~0.9 nm^3. In addition, the 5-hydroxy- and 5-methoxynanoball derivatives are soluble in a variety of organic solvents including alcohols, dimethylformamide, and acetonitrile. More recently, larger

(6) (a) Moulton, B.; Zaworotko, M. J. *Chem. Rev.* **2001**, *101* (6), 1629−1658. (b) MacGillivray, L. R.; Subramanian, S.; Zaworotko, M. J. *Chem. Commun.* **1994**, 1325−1326. (c) James, S. L. *Chem. Soc. Rev.* **2003**, *32* (5), 276−288. (d) Rowsell, J. L. C.; Yaghi, O. M. *Microporous Mesoporous Mater.* **2004**, *73* (1−2), 3−14. (e) Janiak, C. *Dalton Trans.* **2003**, *14*, 2781−2804. (f) Kitagawa, S.; Kitaura, R.; Shin-ichiro, N. *Angew. Chem., Int. Ed.* **2004**, *43* (18), 2334−2375. (g) Kepert, C. J. *Chem. Commun.* **2006**, 695−700.

(7) (a) Zaworotko, M. J. *Chem. Commun.* **2001**, 1−9. (b) Liu, Y.; Kravtsov, V. Ch.; Larsen, R.; Eddaoudi, M. *Chem. Commun.* **2006**, 1488−1490. (c) Eddaoudi, M.; Moler, D. B.; Li, H. L.; Chen, B. L.; Reineke, T. M.; O'Keeffe, M.; Yaghi, O. M. *Acc. Chem. Res.* **2001**, *34* (4), 319−330. (d) Blake, A. J.; Champness, N. R.; Hubberstey, P.; Li, W. S.; Withersby, M. A.; Schröder, M. *Coord. Chem. Rev.* **1999**, *183*, 117−138. (e) Batten, S. R.; Robson, R. *Angew. Chem., Int. Ed.* **1998**, *37* (11), 1460−1494. (f) Jiang, G.; Bai, J.; Xing, H.; Li, Y.; You, X. *Cryst. Growth Des.* **2006**, *6* (6), 1264−1266. (g) Park, K. S.; Ni, Z.; Cote, A. P.; Choi, J. Y.; Huang, R.; Uribe-Romo, F. J.; Chae, H. K.; O'Keeffe, M.; Yaghi, O. M. *Proc. Natl. Acad. Sci. U.S.A.* **2006**, *103* (27), 10186−10191. (h) Perry, J. J.; McManus, G. J.; Zaworotko, M. J. *Chem. Commun.* **2004**, 2534−2535. (i) Chui, S. S. Y.; Lo, S. M. F.; Charmant, J. P. H.; Orpen, A. G.; Williams, I. D. *Science* **1999**, *283* (5405), 1148−1150. (j) Seo, J. S.; Whang, D.; Lee, H.; Jun, S. I.; Oh, J.; Jeon, Y. J.; Kim, K. *Nature* **2000**, *404* (6781), 982−986. (k) Evans, O. R.; Lin, W. *Acc. Chem. Res.* **2002**, *35* (7), 511−522. (l) Biradha, K.; Sarkar, M.; Rajput, L. *Chem. Commun.* **2006**, 4169−4179.

(8) (a) Leininger, S.; Olenyuk, B.; Stang, P. J. *Chem. Rev.* **2000**, *100* (3), 853−907. (b) Seidel, S. R.; Stang, P. J. *Acc. Chem. Res.* **2002**, *35* (11), 972−983. (c) Fujita, M.; Umemoto, K.; Yoshizawa, M.; Fujita, N.; Kusukawa, T.; Biradha, K. *Chem. Commun.* **2001**, 509−518. (d) Caulder, D. L.; Raymond, K. N. *Acc. Chem. Res.* **1999**, *32* (11), 975−982. (e) Tominaga, M.; Suzuki, K.; Kawano, M.; Kusukawa, T.; Ozeki, T.; Sakamoto, S.; Yamaguchi, K.; Fujita, M. *Angew. Chem., Int. Ed.* **2004**, *43* (44), 5621−5625. (f) Sudik, A. C.; Millward, A. R.; Ockwig, N. W.; Cote, A. P.; Kim, J.; Yaghi, O. M. *J. Am. Chem. Soc.* **2005**, *127* (19), 7110−7118.

(9) Steinfeld, J. I. *Molecules and Radiation*; The MIT Press: Cambridge, MA, 1986.

(10) Solomon, E. I. *Inorg. Chem.* **2006**, *45* (20), 8012−8025.

(11) Cotton, F. A.; Walton, R. A. *Multiple Bonds Between Metal Atoms*; Oxford University Press: Oxford, 1982.

(12) (a) Moulton, B.; Lu, J.; Mondal, A.; Zaworotko, M. J. *Chem. Commun.* **2001**, 863−864. (b) Eddaoudi, M.; Kim, J.; Wachter, J. B.; Chae, H. K.; O'Keefe, M.; Yaghi, O. M. *J. Am. Chem. Soc.* **2001**, *123* (18), 4368−4369.

(13) Allen, F. H. *Acta. Crystallogr.* **2002**, *B58*, 380−388.

(14) (a) Abourahma, H.; Coleman, A. W.; Moulton, B.; Rather, B.; Shahgaldian, P.; Zaworotko, M. J. *Chem. Commun.* **2001**, 2380−2381. (b) Mohomed, K.; Abourahama, H.; Zaworotko, M. J.; Harmon, J. P. *Chem. Commun.* **2005**, 3277−3279. (c) Furukawa, H.; Kim, J.; Plass, K. E.; Yaghi, O. M. *J. Am. Chem. Soc.* **2006**, *128* (26), 8398−8399. (d) McManus, G. J.; Wang, Z.; Zaworotko, M. J. *Cryst. Growth Des.* **2004**, *4* (1), 11−13. (e) Ke, Y.; Collins, D. J.; Zhou, H. C. *Inorg. Chem.* **2005**, *44* (12), 4154−4156.

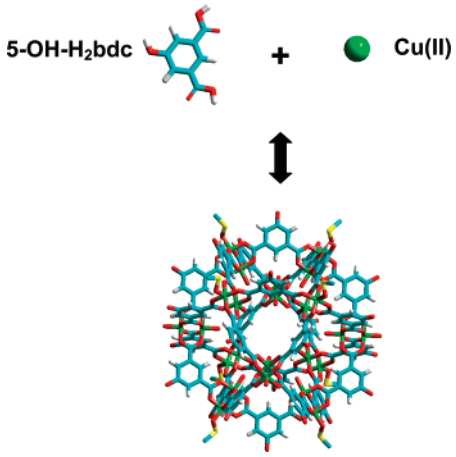

Figure 1. Schematic diagram illustrating the assembly of a discrete OH-nanoball from Cu^{2+} ions and the 5-OH-H_2bdc ligand. The OH-nanoball also contains DMSO solvent molecules coordinated axially to the Cu^{2+} ion in this structure.

pore nanoscale molecules with *cuboctahedron* topology have been synthesized with an $M_{12}L_{24}$ stoichiometry utilizing bis-(4-pyridyl)-based ligands containing acetylene spacers with endohedral functionalization and Pd^{2+} as the metal.[15] Using a similar methodology, porous nanoscale molecules have also been formed using flexible tripodal ligands consisting of *N*,*N*′,*N*″-tris(4-pyridylmethyl)trimesic esters.[16]

Although the solubilities of a number of metal−organic nanoscale molecules in various solvents have been utilized for deposition studies, their corresponding solution properties have not been determined. The fact that these materials have aromatic ligands coordinated to Cu^{2+} metal ions affords an opportunity to explore the photophysical properties of these novel materials. In the present study, the optical properties of Cu^{2+} hydroxylated nanoballs (OH-nanoballs) self-assembled from 5-hydroxybenzene-1,3-dicarboxylate (5-OH-bdc)$^{2-}$ in a methanol solution (Figure 1) were investigated because of their high solubility in alcohols. The results presented here demonstrate the utility of the emission properties of discrete metal−organic structures in probing solution properties including assembly and stability.

Materials and Methods

All reagents were purchased from Sigma-Aldrich and used without further purification. The OH-nanoball was prepared by the addition of 2 equiv of 2,6-dimethylpyridine to a methanolic solution containing equimolar amounts of $Cu(NO_3)_2 \cdot 2.5\ H_2O$ and 5-OH-H_2bdc. This solution was then layered over several milliliters of DMSO to initiate crystallization. The OH-nanoball crystals were collected by filtration and dried prior to use. Formation of the OH-nanoball was verified by single-crystal X-ray diffraction.[14a]

UV/vis spectra were recorded using a Shimadzu UV2401 spectrometer. Steady-state fluorescence measurements were performed with an ISS PC1 (ISS, Inc., Champaign, IL) single-photon-counting spectrofluorimeter. Fluorescence quantum yields were obtained using aniline as a reference ($\Phi = 0.024$ with 300 nm excitation)[17] and

$$\Phi_{5-OH-H_2bdc} = \Phi_{aniline}(I_{5-OH-H_2bdc}/I_{aniline})(n_{5-OH-H_2bdc}{}^2/n_{aniline}{}^2) \quad (1)$$

where I is the total integrated intensity of the given species at $\lambda_{exc} = 300$ nm and n is the solution refractive index. Because all measurements were performed in methanol, it was assumed that $n_{5-OH-H_2bdc} = n_{aniline}$. The integrated intensities (from 325 to 550 nm) were obtained for 5-OH-H_2bdc and aniline solutions having matched optical densities at 300 nm (OD of 0.1 for each). The value for $\Phi_{OH-nanoball}$ was determined in a similar way. Molar extinction coefficients were determined using a calculated molecular weight of 6.61 kDa.

Fluorescence lifetimes were obtained by excitation of the sample with a Continuum Leopard I frequency-quadrupled Nd:YAG laser ($\lambda_{exc} = 266$ nm, <20 ps pulse width, ~40 mW average power with a 20 Hz repetition rate). The emission was collected 90° relative to the excitation path, passed through a 300 nm low-pass filter (Andover Corp. 300FL) and focused onto an Electro-Optics Technologies Inc. ET-2030A amplified photodiode. The output of the photodiode was fed directly into the 50 Ω input of a Tektronix RTDS7404 4 GHz digital oscilloscope.

Electronic structure calculations were performed using the semiemperical ZINDO/S package contained in the ArgusLab suite.[18] The calculations were performed with calculated polarizabilities and configuration interaction involving the lowest eight unoccupied orbitals and the highest eight occupied orbitals. The 5-OH-H_2bdc molecule was first geometry-optimized using an MM+ force field.

NMR spectra were acquired on a Varian Inova at a field strength of 11 T (^{1}H NMR 500 MHz) with a Varian 3 mm indirect detection probe with a single axis gradient at 25 °C (uncorrected). A 45° ^{1}H NMR pulse width of 3.3 μs was followed by a 0.5 s acquisition time and a 1 s relaxation delay. Samples for NMR were dissolved in MeOD and D_2O immediately prior to acquisition.

Results and Discussion

5-OH-H_2bdc. The optical spectrum of 5-OH-H_2bdc in methanol is dominated by an absorption band centered at 312 nm originating from a transition between the ^{1}A′ ground state (C_s symmetry) to an excited state also of ^{1}A′ character (molecular orbital transitions corresponding to 8A′ → 9A′ and 7A″ → 10A″; calculated $\lambda_{max} \sim 302$ nm). Deprotonation of the acid groups of 5-OH-H_2bdc results in (5-OH-bdc)$^{2-}$ with a shift in the absorption band to 301 nm and arises from a transition from the ^{1}A′ ground state to an ^{1}A′ state composed of a mixture of 6A″ → 9A″ and 5A″ → 10A″ orbital transitions (calculated $\lambda_{max} \sim 277$ nm). The molecular orbitals associated with these transitions are displayed in Figure 2. The corresponding emission spectrum of protonated 5-OH-H_2bdc is dominated by an intense band at 355 nm and a weaker band at 440 nm (Figure 3) while the deprotonated (5-OH-bdc)$^{2-}$ results in a shift of the emission maxima to 405 nm. The Stokes shift is also unusually large for the fully deprotonated (5-OH-bdc)$^{2-}$ form being ~111 nm versus ~43 nm for the protonated 5-OH-H_2bdc form. Such large Stokes shifts have been suggested to arise from intermolecular hydrogen bonding. Interestingly, titration of protonated

(15) Tominaga, M.; Suzuki, K.; Murase, T.; Fujita, M. *J. Am. Chem. Soc.* **2005**, *127* (34), 11950−11951.
(16) Ghosh, S.; Mukherjee, P. S. *J. Org. Chem.* **2006**, *71* (22), 8412−8416.
(17) Jameson, D. J.; Croney, J. S.; Moens, P. D. J. Fluorescence: Basic Concepts, Practical Aspects, and Some Anectodes. In *Methods in Enzymology*; Marriott, G., Parker, I., Eds.; Academic Press: New York, 2003; Vol. 360, Part A, pp 1−43,
(18) Thompson, M. A. *ArgusLab 4.0*; Planaria Software LLC: Seattle, WA, http://www.ArgusLab.com.

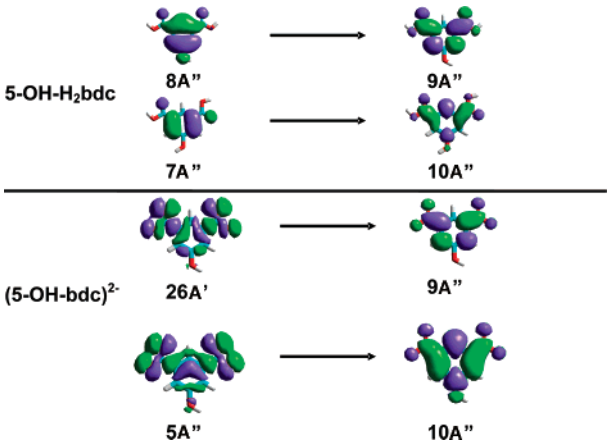

Figure 2. Molecular orbital diagram excitations giving rise to the electronic transitions of both the protonated 5-OH-H_2bdc and deprotonated (5-OH-bdc)$^{2-}$ forms obtained from semiempirical ZINDO/S calculations (see the text for details).

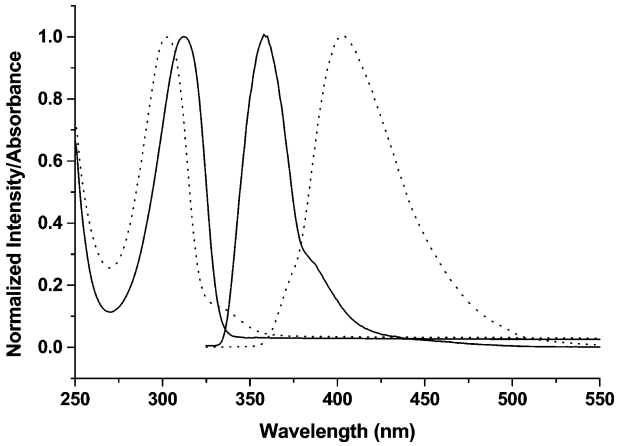

Figure 3. Absorption (<350 nm traces) and uncorrected emission (>350 nm traces) of 5-OH-H_2bdc in methanol (10 μM) with 312 nm excitation in the absence (solid line) and presence (dotted line) of ~0.1 N NaOH. Both the absorption and emission traces were normalized to the maximum intensity for illustrative purposes.

5-OH-H_2bdc with imidazole results in a decrease in the intensity of both the 355 and 440 nm bands but no further increase at 405 nm (Figure 4). This suggests that the two carboxylate groups have different pK_a's, with the first near 4 (pK_a of imidazole) giving a singly deprotonated (5-OH-Hbdc)$^-$ with emission spectra similar to the fully protonated form but with reduced intensity. The fluorescence lifetime is also influenced by the protonation state of the ligand. In the protonated form, the fluorescence lifetime is 1.0 ns while the addition of a base increases the lifetime to 2.3 ns (Figure 4).

The excited-state properties of 5-OH-H_2bdc can be compared to those previously reported for salicylic acid as well as 3-methyl-6-hydroxy-*m*-pthalic acid (MHP) and benzene-1,3-dicarboxylic acid.[19−22] Salicylic acid exhibits an absorption maximum at ~300 nm (concentrations below ~1 μM) with an emission maximum centered at ~430 nm in aprotic solvents. The addition of an appropriate proton acceptor results in a hypsochromic shift in the emission maximum but no significant shift in the UV absorption band. It has been proposed that salicylic acid is capable of both intra- and intermolecular excited-state proton transfer, and this proton-transfer significantly influences the emission spectra of the molecule.[20] The longer wavelength emission band was proposed to arise from an excited-state intramolecular proton transfer between the hydroxyl group and the carbonyl group associated with the neighboring carboxylic acid. Large Stokes shifts have also been observed for *o*-hydroxybenzaldehyde and attributed to excited-state intramolecular proton transfer between adjacent hydroxyl and carbonyl groups.[22] In the case of MHP, the absorption/emission spectra are also dependent upon excited-state intramolecular proton transfer as well as intermolecular hydrogen bonding with either another MHP or solvent (depending upon the solvent hydrogen-bonding capacity).[19,22] The parent MHP exhibits absorption/emission maxima at 325 nm/470 nm due to the excited-state intramolecular proton transfer and 340−350 nm/410 nm for intermolecular hydrogen bonding. These spectra are quite distinct from those of simple benzene-1,3-dicarboxylic acid, which is unable to undergo intramolecular hydrogen bonding (absorption/emission maxima at 290 nm/340 nm).

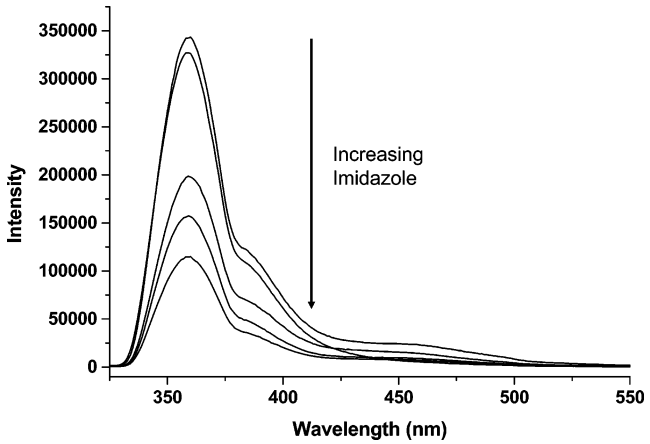

Figure 4. Emission intensity of protonated 5-OH-H_2bdc in methanol in the absence (highest intensity spectrum) and presence of various concentrations of imidazole. The initial concentration of 5-OH-H_2bdc is 10 μM, and the imidazole additions give final concentrations of 1, 2, 5, and 10 mM (in order of decreasing emission intensity).

In the case of 5-OH-H_2bdc, the position of the hydroxyl group precludes intramolecular hydrogen-bonding interactions with the carboxylic acid groups in the 1 and 3 positions. The absorption/emission spectra of 5-OH-H_2bdc are, however, consistent with a fraction of the molecules in solution participating in intermolecular hydrogen bonding either with another 5-OH-H_2bdc or the solvent. The absorption band at 312 nm and the emission band at 355 nm are similar to the absorption/emission spectra of the non-hydrogen-bonded

(19) Das, R.; Mitra, S.; Guha, D.; Mukherjee, S. *J. Lumin.* **1999**, *81*, 61−70.
(20) (a) Denisov, G. S.; Golubev, N. S.; Schreiber, V. M.; Shajakhmedov, S. S.; Shurukhina, A. V. *J. Mol. Struct.* **1997**, *436*−*437*, 153−160. (b) Torlblo, F.; Catalan, J.; Amat, F.; Acuna, A. U. *J. Phys. Chem.* **1983**, *87*, 817−822.
(21) Mandel, A.; Mitra, S.; Banerjee, D.; Bhattacharyya, S. P.; Mukherjee, S. *J. Chem. Phys.* **2003**, *118* (7), 3154−3160.
(22) (a) Nagaoka, S.-I.; Hirota, N.; Sumitani, M.; Yoshihara, K.; Lipczynska-Kochany, E.; Iwamura, H. *J. Am. Chem. Soc.* **1984**, *106*, 6913−6916. (b) Nagaoka, S.-I.; Hirota, N.; Sumitani, M.; Yoshihara, K. *J. Am. Chem. Soc.* **1983**, *105*, 4220−4226.

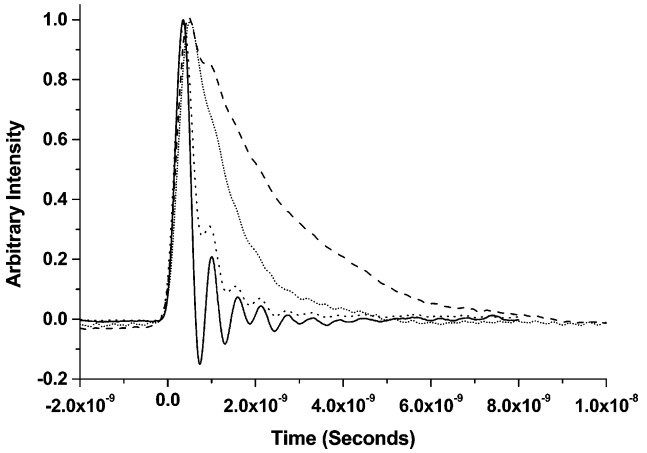

Figure 5. Emission decays for 5-OH-H_2bdc (10 μM) in methanol in the absence (dashed trace) and presence (dot-dashed trace) of 0.1 N NaOH as well as the OH-nanoball (~100 μM; dotted trace) and laser pulse (solid trace). The traces represent the decay of the average emission intensity for wavelengths longer than ~300 nm.

benzene-1,3-dicarboxylic acid, while the 440 nm emission band is near that observed for the intermolecular hydrogen-bonded form of MHP (410 nm). Deprotonation of the carboxylate groups results in perturbations to the electronic structure giving rise to the hypsochromic shift in the absorption band from 312 to 300 nm (originating from the 26A′ → 9A″ and 56A″ → 10A″ orbital transitions) as well as the corresponding emission band (from 355 to 333 nm). However, the large Stokes shift (~111 nm) suggests increased intermolecular hydrogen-bonding interactions between either solvent molecules or another 5-OH-H_2bdc in solution.

$[Cu_2(5\text{-OH-bdc})_2L_2]_{12}$. The optical spectrum of the OH-nanoball in methanol is displayed in Figure 5. The spectrum is dominated by the absorbance of the ligand centered at ~305 nm (ϵ = 83 mM^{-1} cm^{-1}) and a much weaker absorbance centered at 695 nm (ϵ = 7 mM^{-1} cm^{-1}). The position of the ligand absorption band is consistent with the deprotonated $(5\text{-OH-bdc})^{2-}$, which exhibits an absorption maximum at 303 nm. The absorption band centered at 695 nm is in a position indicative of orbitally forbidden Cu d−d transitions or possibly metal−ligand charge-transfer interactions. Semiempirical ZINDO/S calculations of the dicopper tetrakis(*p*-hydroxybenzoate) discrete paddlewheel (representing a less computationally demanding model for the $[Cu_2(5\text{-OH-bdc})_2L_2]_{12}$) suggest that the 695 nm band is primarily composed of several overlapping absorption bands (815, 783, and 708 nm, all having significant contributions from Cu $3d_{xz,yz}$ to ligand-centered π-orbital transitions). In contrast, $Cu^{2+}(NO_3)_2$ in methanol displays only a broad transition centered at ~800 nm (presumably an orbitally forbidden Cu d−d transition).

Excitation of the OH-nanoball solubilized in methanol at 300 nm results in a weak emission band [$\Phi_{OH-nanoball} = (5.6 \pm 0.5) \times 10^{-5}$] centered at ~360 nm with an even weaker shoulder centered at ~390 nm (Figure 6). These emission features are consistent with deprotonated $(5\text{-OH-bdc})^{2-}$ ligands coordinated to the Cu^{2+} center. It is also noted that the emission intensity of the OH-nanoball is several orders

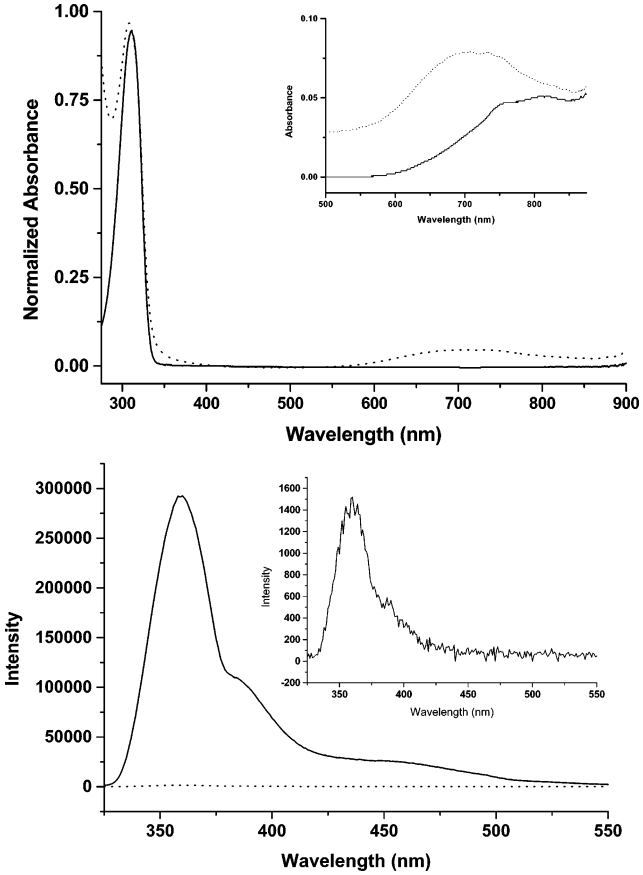

Figure 6. Top panel: Overlay of the absorption spectra of the protonated 5-OH-H_2bdc (solid line) and OH-nanoball (dotted line) in methanol. The inset displays an overlay in the visible region of $Cu^{2+}(NO_3)_2$ (solid line) and OH-nanoball (dotted line) in methanol. Bottom panel: Overlay of the emission spectra of the protonated 5-OH-H_2bdc (solid line) and OH-nanoball (dotted line) in methanol. The concentrations were adjusted such that the optical densities at the excitation wavelength (312 nm) were equivalent for both the 5-OH-H_2bdc and OH-nanoball. Inset: Expansion of the intensity scale for the emission spectrum of the OH-nanoball.

of magnitude weaker than the parent ligand, suggesting significant excited-state quenching within the nanoball complex. This is most likely due to interactions between the π molecular orbitals on the $(5\text{-OH-bdc})^{2-}$ ligand and the Cu^{2+} $3d_{xz,yz}$ orbitals that also give rise to the charge-transfer state discussed above (based upon ZINDO/S calculations). The addition of a weak base such as imidazole results in an increase in the fluorescence associated with the OH-nanoball as expected if the imidazole competes with the $(5\text{-OH-bdc})^{2-}$ carboxylates for coordination sites on the Cu^{2+} ion, resulting in degradation of the OH-nanoball into the deprotonated $(5\text{-OH-bdc})^{2-}$ and $Cu^{2+}(L)_x(L')_y$ complexes [L = deprotonated $(5\text{-OH-bdc})^{2-}$; L′ = imidazole] (Figure 7).

Fluorescence polarization measurements for both deprotonated $(5\text{-OH-bdc})^{2-}$ and the OH-nanoball have also been obtained in order to probe the intactness of the OH-nanoball in methanol. The polarization for the deprotonated $(5\text{-OH-bdc})^{2-}$ ligand (λ_{exc} = 300 nm; λ_{em} = 360 nm) in methanol is 0.038 ± 0.004, which is consistent with the relatively long lifetime (~2 ns) and an emission dipole moment close to that of the absorption dipole moment (i.e., P_0 ~ 0.5). In contrast, the polarization value for the OH-nanoball is 0.066 ± 0.02, which is nearly identical (within experimental

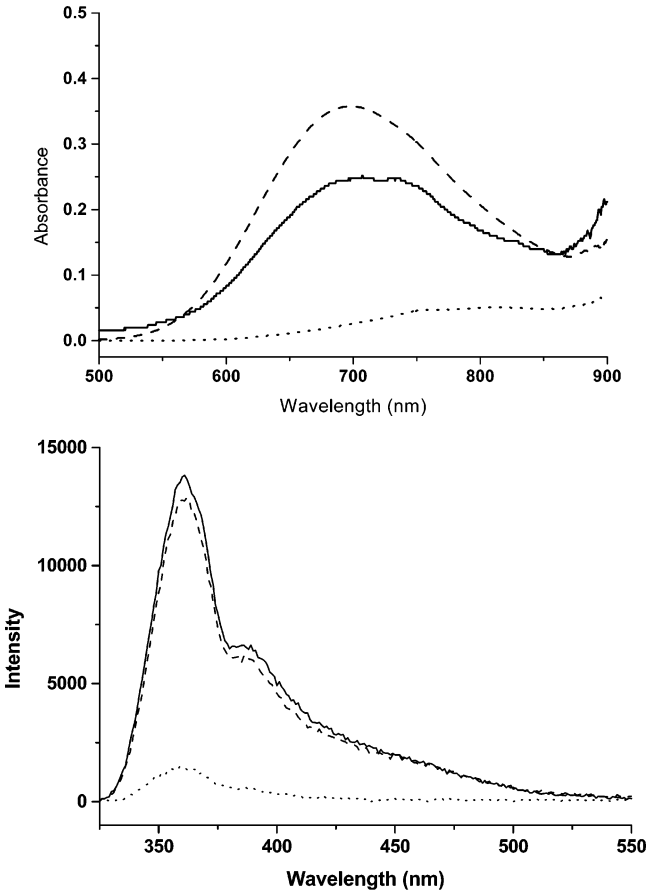

Figure 7. Top panel: Overlay of the absorption spectra of equimolar $Cu^{2+}(NO_3)_2$ and 5-OH-H_2bdc in the absence of aniline (dotted line), equimolar $Cu^{2+}(NO_3)_2$, and 5-OH-H_2bdc in the presence of 2 equiv of aniline (dashed line), and OH-nanoball solubilized from crystals obtained in DMSO (solid line). All spectra were obtained in methanol. Bottom panel: Overlay of the emission spectra of 5-OH-H_2bdc in the absence (solid line) and presence (dashed line) of $Cu^{2+}(NO_3)_2$ in methanol (312 nm excitation). The emission spectrum of 5-OH-H_2bdc, with $Cu^{2+}(NO_3)_2$ indicating the formation of the OH-nanoball, is shown in the dotted trace. Concentrations of 5-OH-H_2bdc and $Cu^{2+}(NO_3)_2$ were 10 μM, while the concentration of aniline was 20 μM.

uncertainty) with that of the free ligand. The polarization, P, is related to the molecular volume of the fluorophore (V) as well as its natural lifetime and limiting polarization (P_0) through eq 2, where η is the solvent viscosity, T is the

$$\frac{1}{P} - \frac{1}{3} = \left(\frac{1}{P_0} - \frac{1}{3}\right)\left[1 + \left(\frac{RT}{V\eta}\right)\tau\right] \qquad (2)$$

temperature, and R is the universal gas constant.[17] Assuming that the limiting polarization (i.e., P_0) of the ligand is not significantly perturbed in the OH-nanoball, then the expected polarization value of the OH-nanoball should be much larger than that of the free ligand because the molecular volume is significantly larger for the OH-nanoball complex and the lifetime is reduced by nearly 1 order of magnitude. Thus, the similarity in the polarization values between the free ligand and the OH-nanoball would suggest that the OH-nanoball might not be intact in a methanol solution. However, the $(5\text{-OH-bdc})^{2-}$ ligands are symmetrically distributed within a spherical supermolecular complex. If the absorbed excitation energy could be rapidly redistributed among the

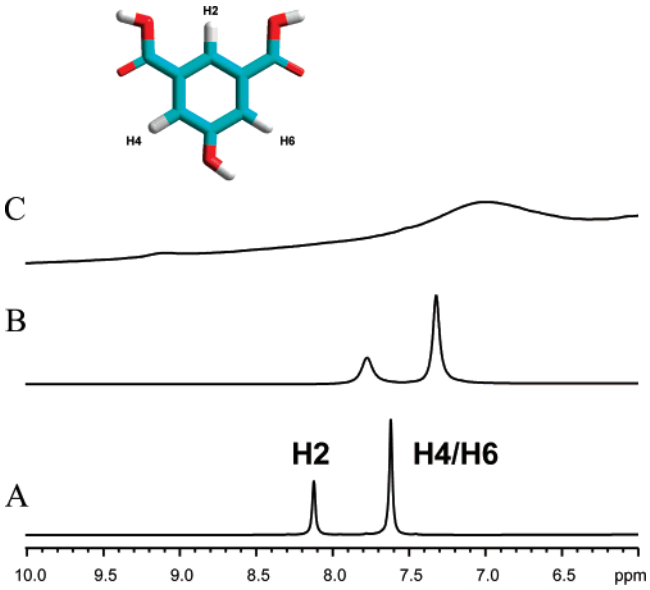

Figure 8. ^{1}H NMR spectra of 5-OH-H_2bdc (~5 mM) (A), 5-OH-H_2bdc + $Cu^{2+}(NO_3)_2$ (~5 mM each) (B), and OH-nanoball (~10 mM) (C) in deuterated methanol. Spectral conditions are described in the Materials and Methods section.

$(5\text{-OH-bdc})^{2-}$ ligands within the spherically symmetric complex, the polarization value would be expected to be that of the free ligand because the net emission dipole of the OH-nanoball would in effect be spherically distributed. This argument is supported somewhat by the higher polarization values of the OH-nanoball after the addition of low concentrations (i.e., millimolar) of imidazole. Under these circumstances, the polarization increases to 0.147 ± 0.006 (as well as the integrated fluorescence intensity) presumably because of the breakdown of the symmetric nanoball structure. In the presence of imidazole, only $[Cu_2(5\text{-OH-bdc})_4]$ fragments as well as various $Cu/(5\text{-OH-bdc})^{2-}$/imidazole coordination complexes would exist.

Monitoring OH-Nanoball Formation in Solution. The spectroscopic properties of the parent 5-OH-H_2bdc ligand as well as the OH-nanoball allow for the monitoring of OH-nanoball formation in solution using either optical absorption or emission spectroscopies. In the case of the absorption spectra, the 695 nm charge-transfer transition appears to be unique to the OH-nanoball. Solutions containing the protonated 5-OH-H_2bdc as well as $Cu^{2+}(NO_3)_2$ in methanol solutions give optical spectra identical with that of $Cu^{2+}(NO_3)_2$ in methanol. The addition of a base (2 equiv of aniline per ligand in this case), which deprotonates 5-OH-H_2bdc, results in the appearance of the 695 nm absorption band and quenching of the ligand emission and anisotropy value identical with that of the OH-nanoball solubilized from single crystals precipitated from a DMSO solution (Figure 7, top). The emission spectrum can also be used to monitor OH-nanoball formation. The emission intensity of the protonated 5-OH-H_2bdc in the presence of $Cu^{2+}(NO_3)_2$ is only slightly reduced relative to the protonated 5-OH-H_2bdc in methanol due to diffusional quenching (Figure 7, bottom). The addition of a base (aniline) results in a significant decrease in the 5-OH-H_2bdc emission intensity consistent with deprotonation of the 5-OH-H_2bdc and subsequent formation of the OH-

nanoball. The corresponding anisotropy of the solution-prepared OH-nanoballs is also identical with that of the DMSO-crystallized/resolubilized species.

Preliminary NMR Studies. Preliminary ^{1}H NMR studies of the $[Cu_2(5\text{-OH-bdc})_2L_2]_{12}$) nanoball dissolved in MeOD exhibit broadening of the 2, 4, and 6 protons of the 5-OH-H_2bdc ligand (see Figure 8). The parent ligand in MeOH exhibits chemical shifts at 8.1 and 7.64 ppm and originates from the H2 proton and H4/H6 protons, respectively. In the presence of Cu^{2+} without added base, the proton resonances are shifted to ~7.8 and ~7.3 ppm and are significantly broadened relative to the free ligand in MeOD. The corresponding ^{1}H NMR spectrum of the OH-nanoball displays a very broad resonance at ~9 and ~7 ppm, and no resonances are observed at ~7.8 or ~7.3 ppm, suggesting there is little or no free ligand in solution.

Summary

Overall these studies demonstrate that OH-nanoballs possess unique optical properties that can be utilized to probe the OH-nanoball structure as well as its formation in methanol solutions. Both the optical absorption and emission spectra clearly indicate significant electronic interaction between the metal-centered d orbitals and ligand-centered π-type molecular orbitals. This is manifested in a long-wavelength charge-transfer transition as well as significant emission quenching and excitation energy redistribution. The polarization measurements clearly indicate that the OH-nanoball retains spherical-type symmetry in solution. Taken together, these represent the first spectroscopic studies of intact OH-nanoballs in solution and provide a framework with which to investigate other intra/intermolecular interactions with this type of discrete metal−organic material.

Acknowledgment. The authors acknowledge the National Science Foundation (Grant MCB-0317334 to R.W.L. and Grant DMR-0101641 to M.J.Z.) and the Petroleum Research Fund (43423-AC4 to R.W.L.) for support of this work.

IC062268I